Ultrashort Pulse Laser Surface Texturing for Injection Mold Functionalization

Andreas Gruner*, Joerg Schille, and Udo Loeschner

Laserinstitut Hochschule Mittweida, University of Applied Sciences Mittweida
Technikumplatz 17, 09648 Mittweida, Germany
**Corresponding author's e-mail: gruner@hs-mittweida.de*

Micro texturing of injection molds for plastic part functionalization has been of growing interest in recent years. Especially for laser texturing it has been successfully demonstrated at lab scale that microscopic surface features can be replicated in plastics at highest structural precision. This paper focusses on high-rate laser surface texturing of injection mold steel 40CrMnMo7 for injection molding of plastic parts with hydrophobic surface behavior. In this study, an ultrashort pulse laser system was used providing an average maximum laser power of 70 W. At first, the most important process parameters like fluence (0.37 – 2.87 J/cm²) and pulse repetition frequency (PRF, 2 – 16 MHz) were varied in order to determine optimal parameter settings for high quality and high throughput laser machining using a polygon scan system with a scanning speed of 100 m/s. In addition, the influencing effect of the microstructure topography on hydrophobicity was examined. Particularly, the laser texturing of the mold sidewalls was challenging as the processing angle was tilted to 45° that was helpful for defect-free demolding of the injection molded 3D-part. Finally, a whole 3D-injection mold was laser textured for injection molding of a small plastic box with a processed surface area > 40 cm² to prove the feasibility of the process.

DOI: 10.2961/jlmn.2024.01.2003

Keywords: ultrashort pulse laser, laser surface texturing, laser direct patterning, injection mold functionalization, micro processing, high pulse repetition frequency (high PRF)

1. Introduction

Laser micro processing of metals using ultrashort pulse laser sources is widely investigated over the last decades and the advantages of ultrashort pulses in micro fabrication are well demonstrated in numerous studies. However, to meet industrial interest regarding short processing times and large area production, there is still a need to scale up processing speed and productivity for high throughput laser machining. Therefore, high-rate laser processing seems to be a promising technology by applying high-power lasers in combination with ultrafast laser beam deflection systems [1]. In a recent approach, it has been demonstrated that high-rate laser processing for direct laser surface texturing is well suitable to provide advanced tribological functionalities on technical surfaces [2]. But nevertheless, direct laser processing and also high-rate laser processing is very time and cost consuming.

As an alternative, laser texturing of tools for replication processes came up as a feasible method for the mass production of functionalized parts and products. For example, recent studies examined whether LIPSS can be transferred to plastic parts by means of injection molding to obtain hydrophobic surface properties [3-7]. In addition, replication of LIPSS on large surfaces by injection molding showed the feasibility of the process [8]. Besides laser processing there are of course competing methods to replicate micro- and nanostructures for surface functionalization, for example EUV-interference lithography [9]. What all above processes have in common is the fact that only flat surfaces were examined, no realistic injection mold part.

The approach of this study is to combine both methods: high-rate laser processing using a high-power ultrashort pulse laser and injection molding for mass production of functionalized plastic parts. Thereby, the focus was on replication not only of LIPSS but also on microstructures at sub-mm scale to provide hydrophobic surface properties. Another challenge was to transfer the microscale surface features onto the sidewalls of the mold. Finally, the laser textured mold was tested in injection molding for mass production of fully functionalized plastic containers including hydrophobic performance demonstration of all inner container surfaces.

2. Experimental setup

In this study, an ultrashort pulse laser system (FX200, Edgewave GmbH) based on InnoSlab technology was used. The laser source delivered a beam of 70 W maximum average laser power and up to 48.72 MHz pulse repetition frequency (PRF) (measured at the sample surface), near Gaussian intensity distribution (M^2 = 1.3) and 1030 nm central wavelength. The initially linearly polarized laser beam was aligned through a quarter wave plate to obtain circular polarization state, which was used for all conducted experiments. The circularly polarized laser beam was ideal for achieving uniform 2.5d ablation structures [10].

The pulse duration was measured with the frequency resolved optical gating method (FROGscan, MesaPhotonics). Figure 1 shows the pulse duration as a function of PRF. The shortest pulse duration of 650 fs was measured at 2 MHz, steadily increasing to 1.2 ps at 48.72 MHz PRF.

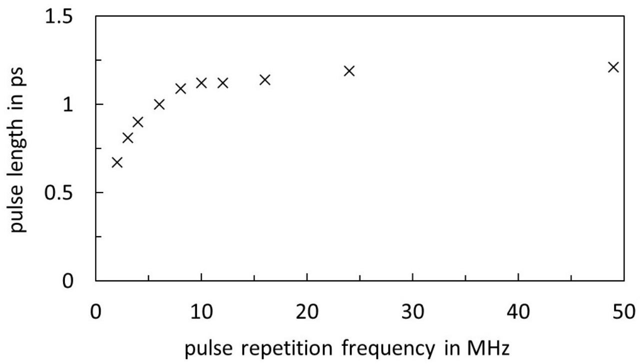

Fig. 1 Pulse duration as a function of the pulse repetition frequency.

For laser beam deflection, a polygon mirror-based scan system was utilized allowing high-speed 2d raster scanning with up to 500 m/s scan speed. The operating principle of the polygon scanner is illustrated in figure 2. The scan system consisted of a double cone polygon wheel for ultrafast laser beam movement in fast axis direction, and a galvanometer scanner for feed motion in slow axis direction. By multiple over scanning the substrate surface with this line-by-line raster scan regime 2.5d microstructures could be produced. All experiments were conducted at a constant scan speed of 100 m/s in fast axis and 5 µm line distance in slow axis.

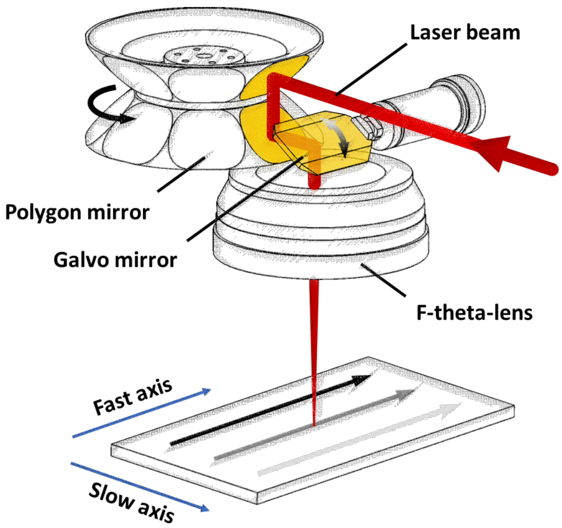

Fig. 2 Operating principle of the polygon scan system.

The laser beam was focused onto the material surface by using an f-theta objective with a focal length of 255 mm. The focal spot diameter and Rayleigh length were measured of 52 µm and 1.4 mm, respectively. The maximum peak fluence of the laser pulses was 2.9 J/cm² as obtained at 1.95 MHz PRF. According to equation (1), the peak fluence decreased linearly with increasing PRF due to the limited average laser power.

$$H_{max} = \frac{2\, P_{av}}{\pi\, w_0^2\, f} \qquad (1)$$

The experimental approach was to laser texture injection molds with goal to get functionalized injection molded plastic parts providing hydrophobic surface behavior. Furthermore, in order to achieve highest processing rate and throughput, the maximum available laser power was applied throughout the study.

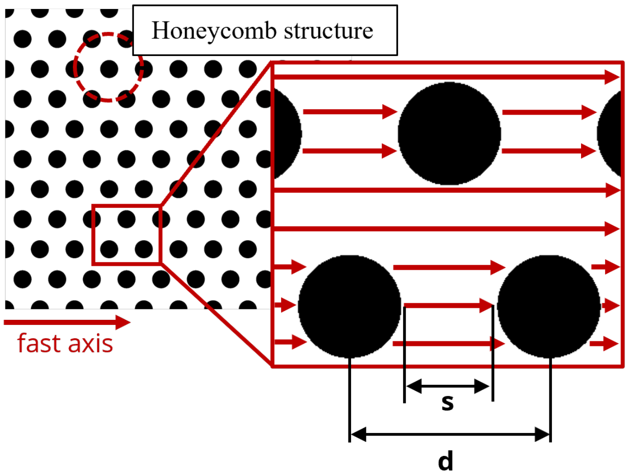

Fig. 3 Desired microstructure: circular pillar pattern with hexagonal orientation; d = pillar distance, s = pillar spacing.

The desired microstructure on the mold surface was a circular pillar pattern with hexagonal orientation to achieve hydrophobic plastic surface [11-12]. The ratio of the pillar diameter and the spacing s between the pillars was fixed to 1 (see figure 3). This led to a honeycomb-like structure on the surface of the injection molded plastic parts.

The investigated mold material was a 40CrMnMo7 mold steel (P20). The polymer for the injection molding process was Polypropylene PPC66A typically used for boxes and pails in food grade. The melt flow rate of the polymer was 20 g/10 min at 230°C polymer temperature.

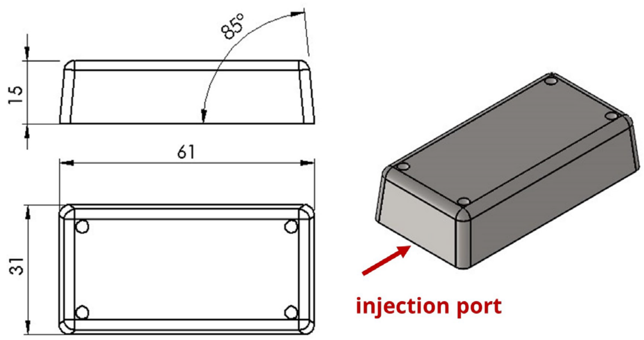

Fig. 4 Mold dimension in mm.

Figure 4 shows the lateral dimension of the laser textured mold. The position of the injection port was at the bottom of the mold, as indicated in fig. 4, right. At all times during the parameter study, the laser beam was directed from the top to the mold. Thereby squares with a field size of 6x6 mm were processed by varying the micro feature dimension. Subsequently the contact angle (CA) of the injection molded plastic part was determined for validation of the intended hydrophobicity. Afterwards, the most suitable surface features were transferred to the sidewall of the mold. Thereby, the molds were laser textured using a 45° tilting angle between the laser beam and the mold walls. This was to produce tilted functional features on the mold walls for reducing mechanical stresses and demolding failure during the demolding of the plastic part [13]. Finally, to demonstrate the feasibility of the process, a whole mold including the top side and the sidewalls was laser textured to injection mold plastic boxes with hydrophobic surface properties even inside the box.

For the injection molding of the plastic boxes, injection molding parameter sets were applied as shown in table 1 [14] by using a BOY 25 E injection molding machine. The applied parameter sets were proved feasible for reliable injection molding of laser processed molds. Afterwards demolding and before wetting tests, the plastic boxes were cleaned 5 minutes in an ultrasonic bath.

Table 1 Injection molding parameter settings.

Temperature in °C	Injection Pressure in MPa	Holding time in s	Filling rate in cm³/s
230	55	8	48

The contact angle was determined by applying water droplets with a volume of 4 µl using the measuring system OCA 15EC (dataphysics). For statistical evaluation, 5 measurements of each parameter were carried out on each functionalized surface.

3. Results and discussion

3.1 Optimal processing parameter

At first, optimal laser parameter settings were identified for maximum ablation and high surface quality. Therefore, a test patch was processed by varying PRF. The pillar distance was set to 200 µm and the number of scan repetitions to 230. So, due to the constant scanning speed of 100 m/s and line distance of 5 µm, the total optical energy irradiated per unit area was constant for all studied parameter sets given in table 2.

Table 2 Investigated laser parameter.

Pulse repetition frequency in MHz	Peak fluence in J/cm²	Pulse distance in µm
2	2.87	50
3	1.87	33.3
4	1.42	25
5	1.19	20
6	0.96	16.7
8	0.73	12.5
10	0.61	10
12	0.49	8.3
16	0.37	6.25

Figure 5 depicts the results of the laser parameter study. The maximum ablation depth and the average ablation volume, as achieved for that specific pillar microstructure were evaluated. On the one hand, the ablation depth is defined by the maximum distance in z-direction from the top of the pillars and the bottom between the pillars. On the other hand, the average ablation volume is given by the measured ablation volume in relation to the measured surface. Both values show similar behavior: Starting with 2 MHz PRF, the curve is increasing to a maximum value, such as 102 µm at 8 MHz (ablation depth) and 70.8 µm³ at 6 MHz (ablation volume) and decreases with higher PRF. An explanation for the slight difference for the maximum values of the curves is that with higher pulse repetition frequency and respective lower fluence the ablation pressure is too low to evaporate, or rather eject the melt completely leading to deposition of the ablated material on the pillar sidewall. So, the optimal parameter for high material removal rate is at 6 MHz and a respective fluence of about 1 J/cm², therefore all further experiments were conducted with this parameter set.

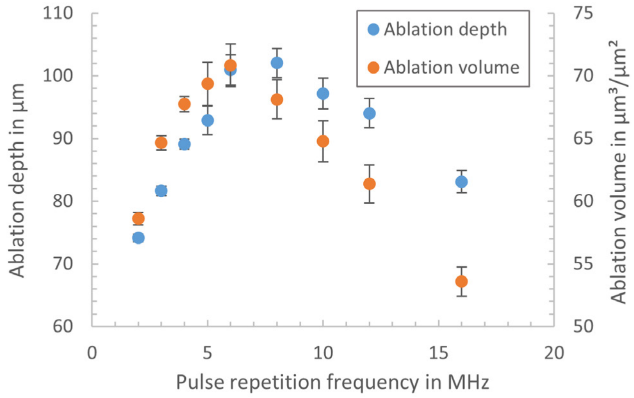

Fig. 5 Average ablation depth and ablation volume dependent on the pulse repetition frequency and respective fluence. The ablation volume is normalized to an area of 1 µm².

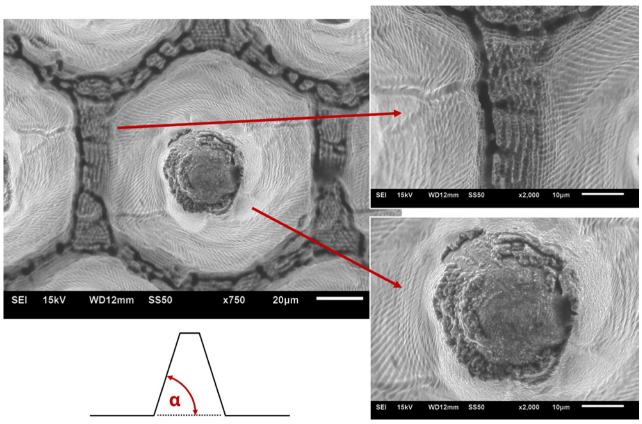

Fig. 6 SEM image of a pillar structure processed with a PRF of 6 MHz and a respective fluence of about 1 J/cm².

To evaluate the quality of the microstructures, figure 6 depicts SEM images of pillars produced with 6 MHz PRF and 1 J/cm² fluence. First of all, characteristic ripples or LIPSS [15] could be observed all over the surface. However, the period of the LIPSS developing on the bottom is different from that appearing on the mold sidewall. This might be due to the fact that the spot size is large in relation to the originating microstructures. As a consequence, permanent reflection of beam parts from the pillar sidewall can be assumed during laser process, in turn, inducing interference effects and subsequent origin of multi-scale surface features.

The sidewall angle α of the pillars was measured in the range between 70° < α < 75°. The topographic analysis of the laser produced pillar structures revealed a high reproducibility across the full scanning field X mm x Y mm as provided by the chosen optical setup.

3.2 Variation of microstructure distance and height

To identify appropriate microstructure dimension, the pillar distance d and the number of scan repetitions were varied. Afterwards injection mold tests were carried out. Finally, the contact angle of the injection molded plastic parts were determined in the wetting tests as described above.

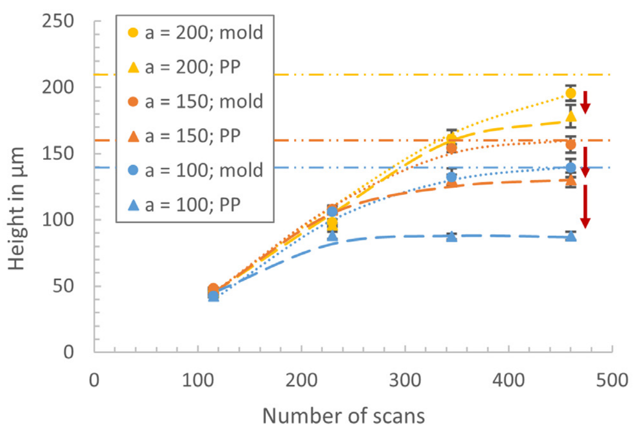

Fig. 7 Pillar height and respective depth of the injection molded plastic part for different pillar distances dependent on the number of scan repetitions. The dotted lines indicate the pillar height of the laser structured mold, and the dashed lines indicate the depth of the replicated honeycomb-structure.

Figure 7 shows the height of the pillar microstructures produced with different number of scan repetitions and lateral pillar distance of 100 µm, 150 µm and 200 µm. In addition, the corresponding depth of the honeycomb microstructure of the injection molded plastic parts is presented. As a general trend, the pillar depth increases with increasing number of scans. This was observed in particular, for the pillars of 150 µm and 200 µm distance. For the shorter pillar distance of 100 µm, however, a height limit of about 140 µm was observed. This might be due to the fact that the pillar base is only somewhat smaller than the pillar distance at this height, that is strongly influenced by the characteristic sidewall angle α. This, in turn, produces narrow trenches between the pillars for higher number of scan repetitions with detrimental effect on material ablation. As another matter of fact, the effective peak fluence of impinging pulses decreased as a result of the enlarging spot size when the larger part of the laser beam irradiates the inclined pillar walls. In addition, a further peak fluence reduction occurred with larger pillar height resulting from defocusing of the laser beam at the deeper processing plane. So, defocusing and inclined processing plane lowered significantly the effective peak fluence and the ablation efficiency suffered. From these results, the limitation of the achievable pillar height can be assessed in a range of 1 to 1.5 of the pillar distance.

Noticeably, depending on the pillar distance there is an obvious mismatch between the height of the laser produced pillars and corresponding plastic replicates. This is indicated in Fig. 7 by the red arrows, showing for the smaller features a greater deviation between the laser textured pillars and replicated plastic microstructures. In optimum case, the size of the pillars and the plastic honeycomb structures should be equal. Accordingly, the detected mismatch between pillar and replicate structure size indicates incomplete polymer penetration towards the bottom of the laser textured mold that is potentially affected by the limited fluidity and melt flow rate of the PPC66A polymer in combination with the used injection molding parameter. This effect is somewhat more pronounced with increasing number of scan repetitions respectively more narrow trenches between the pillar structures. By the example of a pillar distance of a = 100 µm and 460 scan repetitions, the ratio between replication depth (88 µm) in relation to the pillar height (140 µm) is only about 63 %. This ratio increased for the wider features, such as 82 % for a = 150 µm or 91 % for a = 200 µm. This statement is confirmed by representative SEM images showing the mold and respective injection molded plastic parts in Fig. 8. In addition, a higher replication quality of the plastic replicates was obtained with the pillar structures produced at 200 µm distance and 230 scan repetitions. (fig. 8, top images).

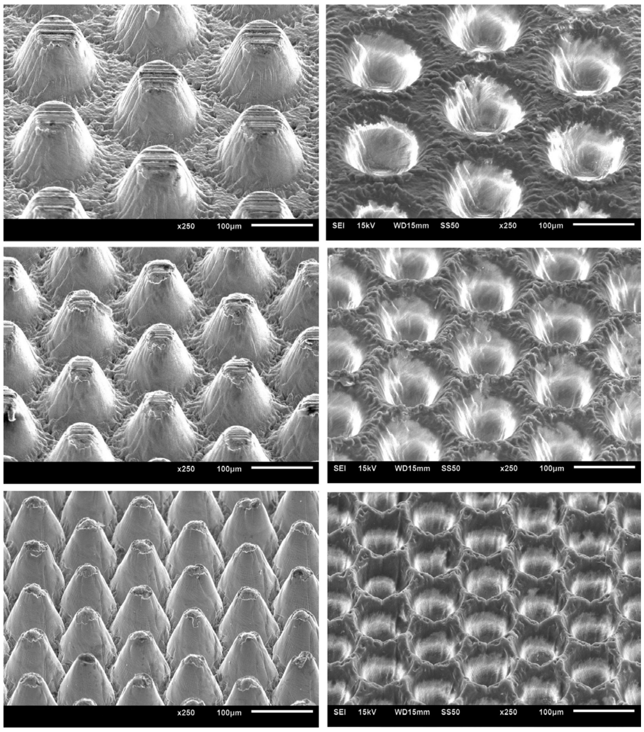

Fig. 8 SEM-images of different pillar distances (left) and the respective injection molded plastic parts (right) for a PRF of 6 MHz, a fluence of 1 J/cm², 230 scan repetitions and a pillar distance of 200, 150 and 100 µm (top down), angle of view: 45°.

In order to provide a more detailed view onto the quality of the injection molded plastic replicates, fig. 9 depicts a SEM image of the honeycomb features. Inside the holes can be seen that the LIPSS originating on mold surface during laser texturing can perfectly be transferred to the plastic parts. On top of the honeycomb microstructure, as can be seen in the region between 3 holes, there are also well replicated LIPSS. But especially for the narrowest region directly between 2 holes there is an incomplete polymer penetration of the bottom of the mold. And crosswise the polymer flow direction there is an incompletely merged area, characterized by a narrow slit, as the polymer solidifies before merging. An explanation therefore is provided by G. Lucchetta et. al. [16], as they investigated the technological limits of micro injection molding by replicating high aspect ratio micro structured surfaces. The authors showed that the mold temperature has a significant influence on the replication degree. Furthermore, they observed a non-uniform pressure distribution leading to micro feature deviation along the cavity.

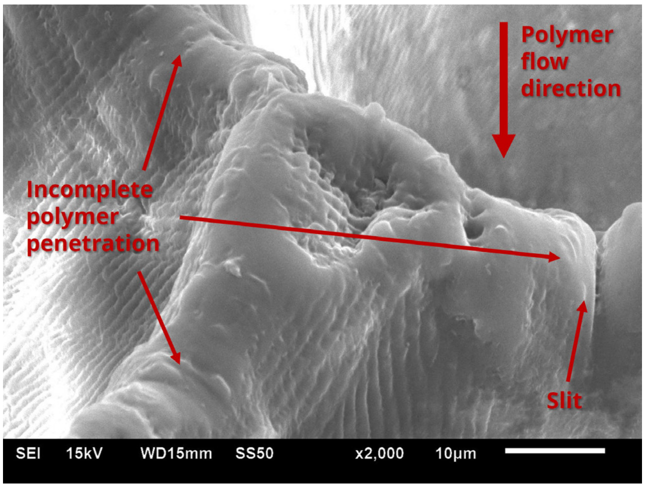

Fig. 9 SEM-image of the honeycomb structure on top of an injection molded plastic part, pillar distance: 100 µm, number of scan repetitions: 230, angle of view: 45°.

3.3 Contact angle measurement

Although the transfer of the microstructure to the injection molded plastic parts was not optimal, contact angle measurements showed the efficacy and functionality of the replicated microstructures. For an untreated plastic surface, the contact angle was measured to 80-90°. For the replicated laser textures, the plastic surfaces provided a significant higher CA reaching up to 130° (figure 10 + figure 11).

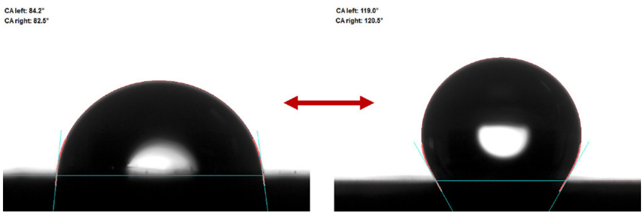

Fig. 10 Contact angle: untreated surface (CA ≈ 83°) vs. laser texture replicated surface (CA ≈ 120°).

Fig. 11 summarizes the measured CA of the plastic parts dependent on the number of scan repetitions and thereby microstructure height for different microstructure distances a. As a general trend, it can be seen, that the CA can be increased by the functionalized plastic surfaces. Thereby, the distance between the functional features has only a marginal influence on the CA. The number of scan repetitions, or rather the aspect ratio between pillar distance and pillar height, had a considerably greater effect on CA. From this, it can be concluded, for every pillar distance there exists an optimal range of the pillar height which in combination with the pillar sidewall angle leads to a narrow bottom between the pillars. In consequence, this reduces the effective surface of the honeycomb structure of the related injection molded plastic part thus providing the hydrophobic surface behavior as verified by the increased contact angles. However, in Fig. 11, high standard deviation bars can be seen which resulted from the fact, that the replicated honeycomb structure quality is not homogeneous enough to provide reliable and repeatable CA-measurement results. Therefore, further investigation of the injection molding process is essential to understand the influence of the pillar microstructure on the injection molding process and finally to evaluate the optimal microstructure dimension of the mold to produce injection molded parts with homogeneous hydrophobic surface properties.

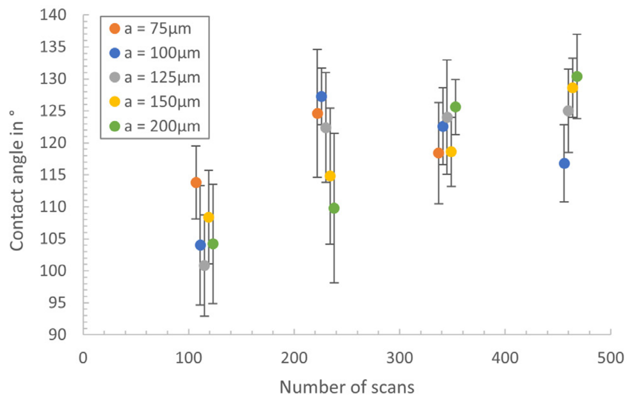

Fig. 11 Contact angle measured on the injection molded plastic part in dependence of the number of scan repetitions and different pillar distances as laser textured on the mold. (The data points are plotted with a little offset to visualize the standard deviation bars).

However, with view onto productivity and throughput, it is advantageous to apply a minimal number of scan repetitions as there is a linear correlation between scan repetitions and the overall processing time. For that reason, a pillar distance of 100 µm in combination with 230 scan repetitions corresponding to a pillar height of about 100 µm seems to be the best deal to achieve appropriate hydrophobic performance at high CA in a reasonable processing time. For that microstructure parameter set the CA was measured to 127.3° ± 4.4°.

3.4 Sidewall processing

Based on these findings presented for the top side laser texturing of the mold, the process was transferred to the sidewall of the mold. Therefore, the mold surface to be processed was tilted 45° relative to the incoming laser beam. Initially, the idea was to apply identical laser parameters as identified optimal for the top side processing (PRF: 6 MHz, pillar distance and height: 100 µm). By doing so, the relative tilting between the mold surface and the laser beam caused an elliptical shaped focus spot that increased the focus spot area that, in turn, lowered the peak fluence of the laser beam in the processing plane to be 0.7 J/cm².

Figure 12 depicts SEM images of the chosen microstructure distance of 100 µm. The pillar quality is similar to ones achieved at the top side and perpendicular laser beam incidence. The pillar microstructure is completely covered with LIPSS, which can be found on the top of the mold as well as on the sidewalls and the mold bottom between the pillars. The CA on the sidewall of the injection molded plastic part of 123.2° ± 2.2° was slightly lower than the one measured on the perpendicular textured surface (127.3° ± 4.4°) mentioned above.

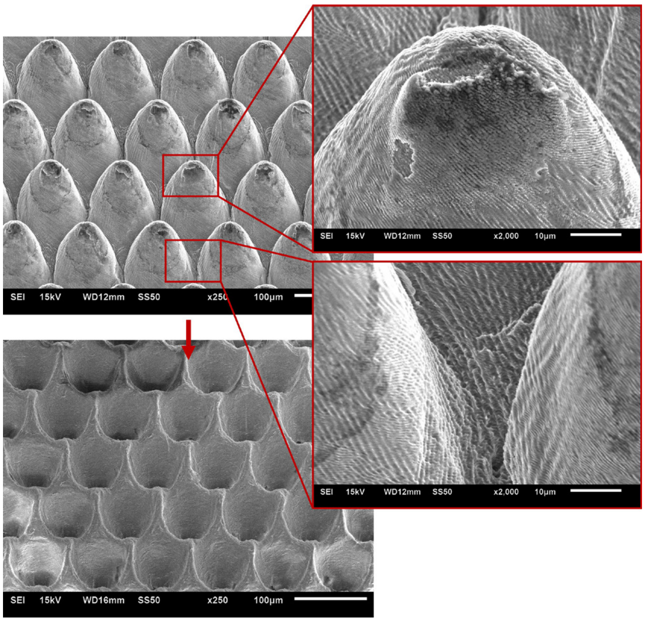

Fig. 12 Sidewall processing using a process tilting angle of 45°: PRF: 6 MHz, fluence: 0.7 J/cm², a = 100 µm, measured CA: 123.2° ± 2.2°.

3.5 Processing of a complete mold

Finally, a real mold was laser textured including the top and sidewalls in order to demonstrate the feasibility and the reliability of laser-based mold functionalization in injection molding applications. The laser textured molds were tested in thermal injection molding with goal to produce small plastic boxes with hydrophobic properties of the inner surfaces (fig. 13).

Fig. 13 Development cycle: original mold (left), laser textured mold (middle), injection molded plastic box (right).

For mold processing, the laser parameters were set as follows: 1 J/cm² fluence on the top side, 0.7 J/cm² on the sidewall, 6 MHz PRF, 100 m/s scan speed, 100 µm pillar distance and pillar height (corresponding to 230 scan repetitions). The processed surface area was about 41 cm² and the total laser processing time was 5 hours. This resulted in an area processing rate of 0.14 cm²/min which is little below the processing rates achieved in a previous study on riblet profiling, where lower structure depths were produced in Aluminum alloy [16]. The demolding of the plastic box was assisted by ejection pins assembled in the injection molding setup. During demolding there occurred mechanical stresses around the ejection pins leading to little material deformation. To reduce this effect, a release agent was applied. Furthermore, deviations in the honeycomb microstructure quality were observed resulting from inhomogeneous wetting of the polymer along the laser textured surface of the whole mold, also described in [16].

For the assessment of the wetting behavior, ten individual CA-measurements were carried out on different positions on the bottom as well as of the sidewall of the injection molded plastic boxes. The average CA on the bottom amounted to 117° ± 2.3° and on the sidewall 107° ± 2.8°. On the one hand, these measured values are not as high as the CA of the test patches. On the other hand, the results obtained provide clear evidence on the higher hydrophobicity of functionalized plastic parts by using laser textured molds. Moreover, with this successful demonstration it can be concluded that laser surface texturing provides a promising alternative for surface functionalization in injection molding.

4. Conclusion and outlook

In this study it is successfully demonstrated that ultrashort pulse laser texturing of injection molds is well suitable to produce functionalized injection molded plastic parts. High throughput machining reaching up to 0.14 cm²/min could be achieved by combining an ultrashort pulse laser beam of 67 W average laser power with an ultrafast polygon scanner-based scan system.

At first, optimal laser processing parameter were identified for efficient mold texturing. Secondly, the microstructure geometry (distance and height) was varied in a wide range by texturing test patches with a dimension of 6 x 6 mm². This was in order to identify the optimum surface texture parameter for hydrophobic behavior of the replicated plastic parts. After injection molding of the textured molds, the contact angles of every test patch were measured, showing that the hydrophobicity could be significantly increased by laser texturing of the mold for functionalization. The next step was to transfer the process on oblique sidewalls to mimic the conditions of 3D real-life products. Therefore, the surfaces to be processed were tilted by an angle of 45° that has been proven as appropriate for damage-free demolding in a preliminary study. Finally, a whole mold was processed using a pulse repetition frequency of 6 MHz, a peak fluence of 1 J/cm² (correlating to 0.7 J/cm² for the sidewall processing due to the tilting angle) and a microstructure distance and height of 100 µm resulting in an injection molded plastic box with a functionalized inner surface. The pillar microstructure of the mold showed a high homogeneity on the entire surface.

However, there some problems occurred as the replication of the microstructure to the plastic part was incomplete especially for the narrow trenches on the bottom between the pillar microstructures. Additionally, for the processing of the whole mold, the feature replication was not homogeneous along the mold. Furthermore, there has been mechanical stress during the ejection of the plastic box leading to slight material deformation around the ejection pins.

All described problems are related to the injection molding process, so there is a need for further investigation of the process to find appropriate injection molding parameters as well as a more suitable polymer to increase the replication quality of the microfeature on the surface of the injection molded part.

As the laser texturing process is scalable by using polygon scan systems for ultrafast laser beam deflection and, further, there is an ongoing trend to higher laser powers reaching kW-levels even for ultrashort pulse lasers, also the productivity in mold laser texturing can be enhanced. Accordingly, large-scale, and high-speed surface texturing will pave the way for the high-rate laser technology to industrial applications in the near future. With view onto mold functionalization addressed in this study, this is welcome to functionalize technical surfaces of m² range in industrial relevant processing times, to provide functionalized molds for mass production of innovative real-life products.

Acknowledgment
The authors thank the M-ERA.NET Network and the sächsische Aufbaubank SAB for funding project no. 100405762.

References
[1] J. Schille, and U. Loeschner: Adv. Opt. Techn. 10, (2021) 233.
[2] J. Schille, L. Schneider, S. Mauersberger, S. Szokup, S. Hoehn, J. Poetschke, F. Reiß, E. Leidich, and U. Loeschner: Lubricants 8, (2020) 33.
[3] P. Hernández, A. Murawko, J. Martínez, G. Peláez, and E. Ares: Procedia Engineering 63, (2013) 885.
[4] X. Wang, H. Zheng, Y. Wan, W. Feng, and Y.C. Lam: Engineering 4, (2018) 816.
[5] L. Piccolo, M. Sorgato, A. Batal, S. Dimov, G. Lucchetta, and D. Masato: Micromachines 11, (2020) 429.
[6] A.H.A. Lutey, G. Lazzini, L. Gemini, A. Peter, V. Onuseit, J. Graus, F. Fuso, R. Kling, and L. Romoli: J. of Manufacturing Processes 65, (2021) 445.
[7] J. Bekesi, J.J.J. Kaakkunen, W. Michaeli, F. Klaiber, M. Schoengart, J. Ihlemann, and P. Simon: Appl. Phys. A 99, (2010) 691.
[8] P.H. Wu, C.W. Cheng, C.P. Chang, T.M. Wu, and J.K. Wang: J. Micromech. Microeng. 21, (2011) 115032.
[9] C. Holzer, J. Gobrecht, H. Schift, and H. Solak: Macromol. Symp. 296, (2010) 316.
[10] K. Venkatakrishnan, B. Tan, P. Stanley, and N.R. Sivakumar: J. of Appl. Phys. 92, (2002) 1604.
[11] J.-M. Romano, M. Gulcur, A. Garcia-Giron, E. Martinez-Solanas, B.R. Whiteside, and S.S. Dimov: Appl. Surface Science 476, (2019) 850.
[12] M. Groenendijk: Laser Technik Journal 5, (2008) 44.
[13] D.G.K. Aboud, A. Gruner, and AM. Kietzig: Appl. Phys. A 128, (2022) 1057.
[14] F. Johannaber: “Injection Molding Machines” (Carl Hanser Publishing, Munich, 2008) p.10.
[15] J. Bonse, S.V. Kirner, and J. Krueger: “Laser-Induced Periodic Surface Structures (LIPSS)” in “Handbook of Laser Micro- and Nano-Engineering” ed. by K. Sugioka (Springer, Cham, 2020) p.879.
[16] G. Lucchetta, M. Sorgato, S. Carmignato, and E. Savio: CIRP Annals 63, (2014) 521.
[17] S. Mauersberger, J. Schille, K. Kujawa, L. Schneider, C. Million, K. Hartung, K. Oehlert, and U. Loeschner: J. of Laser Micro Nanoeng. 15, (2020) 16.

(Received: July 31, 2023, Accepted: December 10, 2023)